



## Rhombic patterns: Broken hexagonal symmetry

Qi Ouyang, Gemunu H. Gunaratne, and Harry L. Swinney

Citation: *Chaos* **3**, 707 (1993); doi: 10.1063/1.165931

View online: <http://dx.doi.org/10.1063/1.165931>

View Table of Contents: <http://scitation.aip.org/content/aip/journal/chaos/3/4?ver=pdfcov>

Published by the [AIP Publishing](#)

---

### Articles you may be interested in

[Active particles with broken symmetry](#)

*Chaos* **21**, 047517 (2011); 10.1063/1.3669493

[Broken symmetries and magnetic dynamos](#)

*Phys. Plasmas* **14**, 102301 (2007); 10.1063/1.2780138

[Broken symmetries in the entanglement of formation](#)

*J. Math. Phys.* **44**, 2402 (2003); 10.1063/1.1570509

[Broken symmetry](#)

*Phys. Teach.* **38**, 564 (2000); 10.1119/1.1341953

[Dissipative structures and broken symmetry](#)

*J. Chem. Phys.* **74**, 755 (1981); 10.1063/1.440794

---



# Rhombic patterns: Broken hexagonal symmetry

Qi Ouyang

Center for Nonlinear Dynamics and Department of Physics, The University of Texas, Austin, Texas 78712

Gemunu H. Gunaratne

Department of Physics, The University of Houston, Houston, Texas 77204

Harry L. Swinney

Center for Nonlinear Dynamics and Department of Physics, The University of Texas, Austin, Texas 78712

(Received 27 August 1993; accepted for publication 29 October 1993)

Landau–Ginzburg equations derived to conserve two-dimensional spatial symmetries lead to the prediction that rhombic arrays with characteristic angles slightly differ from  $60^\circ$  should form in many systems. Beyond the bifurcation from the uniform state to patterns, rhombic patterns are linearly stable for a band of angles near the  $60^\circ$  angle of regular hexagons. Experiments conducted on a reaction–diffusion system involving a chlorite–iodide–malonic acid reaction yield rhombic patterns in good accord with the theory.

## I. INTRODUCTION

Nearly a century ago Bénard observed the formation of a hexagonal array of convection cells in a thin layer of fluid heated from below.<sup>1</sup> Under different conditions convection can also produce a periodic array of rolls<sup>2</sup> or squares.<sup>3</sup> Such periodic arrays of hexagons, stripes (rolls), or squares have been observed to form from the uniform state in a number of physical systems, including garnet layers,<sup>4</sup> ferrofluids,<sup>5</sup> and reaction–diffusion systems.<sup>6,7</sup>

Recently we undertook an experimental study of pattern formation in a reaction–diffusion system, expecting to observe regular periodic arrays of hexagons, as had been reported earlier.<sup>6,7</sup> Instead we found, as Fig. 1(a) illustrates, that the system spontaneously forms multiple domains, each of which contains a fairly uniform rhombic array with characteristic angles near but in general different from  $60^\circ$ ;<sup>8,9</sup> the angle is  $66^\circ$  in the domain shown in Fig. 1(b). The rhombic patterns emerge simultaneously everywhere. This contrasts with the well-studied target and spiral patterns in excitable media, where the patterns are initiated by pace-makers (e.g., a dust particle or an imperfection at the boundary). Histograms of the distribution of angles for patterns observed at two different values of the bifurcation parameter are plotted in Fig. 1(c). The band of observed angles increases in width as the bifurcation parameter is increased beyond the transition to spatial patterns.

The rhombic domains in the extended pattern of Fig. 1(a) appear to be stable. We checked the stability of the patterns by imposing rhombic perturbations with different characteristic angles. If the characteristic angle of the imposed pattern is close to  $60^\circ$ , the pattern remains stationary after the perturbation is removed, indicating the stability of the state. However, if the imposed angle deviates too far from  $60^\circ$ , then the system rearranges after the removal of the perturbation. For given external parameters the characteristic angles of stationary states lie within an interval of angles about  $60^\circ$ .

## II. THEORY

We will show that the existence and stability of the observed patterns can be explained by a Landau–Ginzburg theory constructed purely on the basis of symmetries, and then we will describe experiments that test the theoretical predictions. The theory is built on the assumption that an extended system (where boundary effects can be neglected) is invariant under rigid body motions, i.e., translations, reflections, and rotations. The uniform state with all of these symmetries undergoes spontaneous symmetry breaking leading to patterns. A theory of the loss of translational invariance, presented below, predicts the formation of rhombic patterns. The generality of the Landau–Ginzburg theory suggests that many pattern forming systems should exhibit the same behavior as we have found for a reaction–diffusion system.

We characterize the pattern using a scalar field  $U(\mathbf{x}, t)$ , which vanishes when the system is uniform. For our chemical system,  $U(\mathbf{x}, t)$  could denote the difference between the local concentration and the mean value of one of the chemical species. For surface-tension-driven convection,  $U(\mathbf{x}, t)$  could represent the fluid surface velocity. Prior to the bifurcation the solution  $U(\mathbf{x}, t) = 0$  is stable against all perturbations. The bifurcation produces a characteristic length scale and hence an annulus of unstable modes. For isotropic systems, the resulting pattern  $U(\mathbf{x}, t)$  can be expanded in a *hexagonal planform* as<sup>10,11</sup>

$$U(\mathbf{x}, t) = a_1(\mathbf{x}, t)e^{ik_1 \cdot \mathbf{x}} + a_2(\mathbf{x}, t)e^{ik_2 \cdot \mathbf{x}} + a_3(\mathbf{x}, t)e^{ik_3 \cdot \mathbf{x}}, \quad (1)$$

where  $\mathbf{k}_i$  are a set of hexagonal basis vectors

$$\begin{aligned} \mathbf{k}_1 &= k_0 \mathbf{j}; & \mathbf{k}_2 &= k_0 \left( \frac{\sqrt{3}}{2} \mathbf{i} - \frac{1}{2} \mathbf{j} \right); \\ \mathbf{k}_3 &= k_0 \left( -\frac{\sqrt{3}}{2} \mathbf{i} - \frac{1}{2} \mathbf{j} \right), \end{aligned} \quad (2)$$

and  $a_n(\mathbf{x}, t)$  are slowly varying complex functions called the envelope functions. The envelope functions for uniform rolls parallel to the  $x$  axis are  $a_1 = \text{const}$ ,  $a_2 = a_3 = 0$ ; for a periodic array of hexagons,  $a_1 = a_2 = a_3 = \text{const}$ .

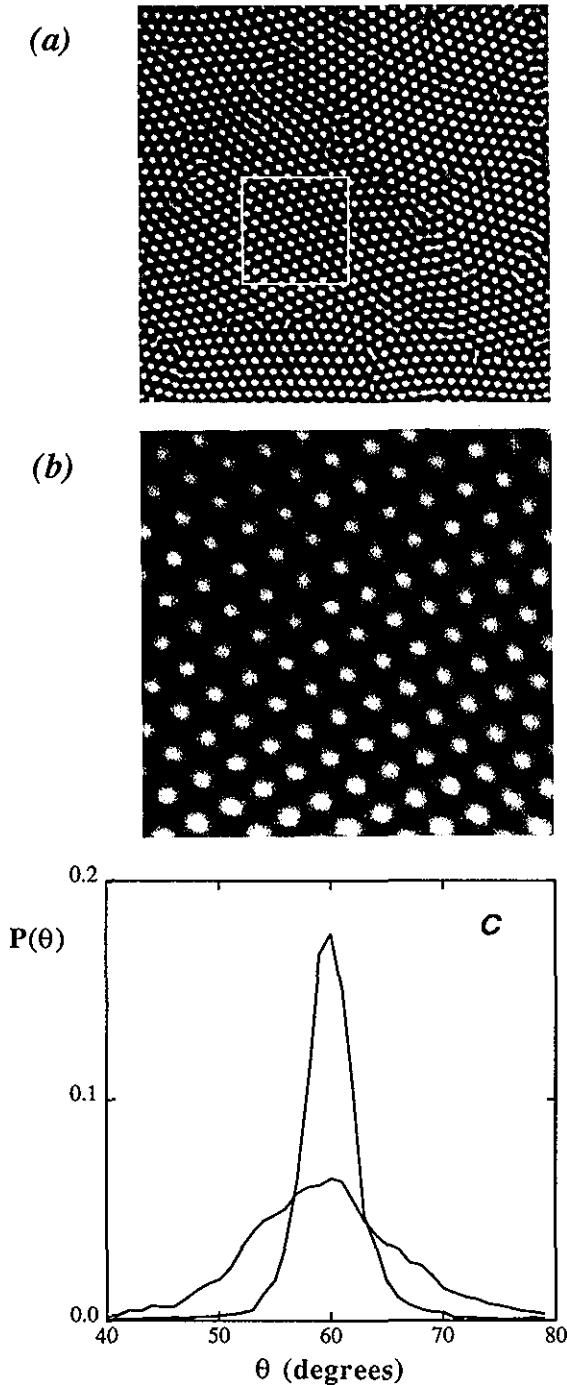


FIG. 1. (a) Extended reaction-diffusion pattern with different characteristic angles in a band near  $60^\circ$ ; the region shown is  $6 \times 6$  mm.<sup>9</sup> (b) Close-up of the region in the box in (a); each dot has nearest neighbors at well-defined angles:  $57^\circ$ ,  $57^\circ$ , and  $66^\circ$ . At first sight the pattern may appear to be hexagonal, but a closer inspection reveals that the hexagons are distorted. This is the signature of a rhombic array. (c) Distribution of angles observed in patterns at two values of the control parameter. The narrow distribution, which has an rms width of  $2.3^\circ$ , was observed not far beyond the onset of patterns; the broad distribution, which has an rms width of  $4.5^\circ$ , was obtained farther away from the transition.

A rhombic array can be obtained by *stretching* a hexagonal array along one of its symmetry axes.<sup>12</sup> We can deduce the form of the resulting envelope functions by applying the transformation

$$S: (x, y) \rightarrow ((1 + \bar{\beta})^{-1} x, y) \quad (3)$$

to a hexagonal pattern. Transformation (3) stretches the  $x$  axis, which is one of the six symmetry axes of the hexagonal array. Substituting in Eq. (1), we deduce that the rhombic pattern  $U_R(x, t)$  can be described as

$$U_R(x, t) = \sum_{n=1}^3 a_n e^{i k_n \cdot (S^{-1} x)}. \quad (4)$$

Since

$$k_1 \cdot (S^{-1} x) = k_1 \cdot x,$$

$$k_2 \cdot (S^{-1} x) = k_2 \cdot x + (\sqrt{3}/2) \bar{\beta} x,$$

and

$$k_3 \cdot (S^{-1} x) = k_3 \cdot x - (\sqrt{3}/2) \bar{\beta} x,$$

the envelope functions for the rhombic array, expanded in the original basis (2), are

$$A_1 = a_1, \quad A_2 = a_2 e^{i \beta x}, \quad A_3 = a_3 e^{-i \beta x}, \quad (5)$$

where  $\beta = (\sqrt{3}/2) \bar{\beta}$ . The envelope function formalism is applicable only if the envelope functions  $A_n$  are slowly varying; thus the theory presented below will hold when  $\beta$  is small.

The qualitative properties of pattern formation, in particular the existence and stability of rhombic arrays, can be studied through a *lowest order* expansion of the dynamics of  $A_n$ 's constructed to retain all the symmetries of the original system. In our case, the dynamics has to preserve the invariance of the system under translations, rotations, and reflections. The resulting spatiotemporal equations (which we refer to as the Landau-Ginzburg equations) are<sup>13</sup>

$$\begin{aligned} \partial_t A_1 &= \gamma \square_1^2 A_1 + \mu A_1 + \alpha \bar{A}_2 \bar{A}_3 \\ &\quad - (|A_1|^2 + \rho |A_2|^2 + \rho |A_3|^2) A_1, \\ \partial_t A_2 &= \gamma \square_2^2 A_2 + \mu A_2 + \alpha \bar{A}_3 \bar{A}_1 \\ &\quad - (|A_2|^2 + \rho |A_3|^2 + \rho |A_1|^2) A_2, \\ \partial_t A_3 &= \gamma \square_3^2 A_3 + \mu A_3 + \alpha \bar{A}_1 \bar{A}_2 \\ &\quad - (|A_3|^2 + \rho |A_1|^2 + \rho |A_2|^2) A_3, \end{aligned} \quad (6)$$

where  $\bar{A}$  is the complex conjugate of  $A$ , and the parameters  $\mu$ ,  $\alpha$ ,  $\rho$ , and  $\gamma$  are real. The spatially invariant part of the equations is the normal form for systems with the required symmetries,<sup>14,15</sup> while the combination of spatial derivatives  $\square_n = [\hat{k}_n \cdot \nabla - (i/2k_0) \nabla^2]$  has been constructed to preserve the rotational invariance of the set of solutions *exactly*.<sup>13</sup> (Here  $\hat{k}_n$  is the unit vector along  $k_n$  and  $k_0$  is the length of each of the vectors  $k_1$ ,  $k_2$ , and  $k_3$ , and  $\nabla$  acts in the plane.) Thus if the pattern  $U(x, 0)$  is rotated by  $R$  to give  $V(x, 0) = U(R^{-1} x, 0)$ , then the dynamics given by Eq. (6) implies that  $V(x, t) = U(R^{-1} x, t)$  for any subsequent time  $t$ .

Equation (6) is different from other spatiotemporal extensions of the normal form<sup>16</sup> in that it preserves the rotational invariance *exactly*. Thus even though the earlier forms of the Landau-Ginzburg equations yield stripes and

hexagons (and also rhombic arrays), those arrays point in certain fixed directions. This cannot be the case for a physical system that is rotational invariant. The multiple-scale analysis of Newell, Whitehead, and Segel<sup>17</sup> leads to amplitude equations that are not rotationally invariant in any finite truncation. Each individual term regains the required rotational invariance when the perturbation is carried out to higher order. Thus at the lowest order in perturbation (of, say, the Swift-Hohenberg equation) the amplitude equations contain "noninvariant" terms like  $(\hat{\mathbf{k}}_n \cdot \nabla)^2 A_n$ . However, on carrying out the perturbation to higher order it is seen that this term is "completed" to the rotationally invariant  $\square_n^2 A_n$ . We will show in a subsequent publication how a multiple scale analysis<sup>17</sup> can be modified to get the combination of spatial derivatives  $\square$  and Eq. (6). Pattern formation in nonvariational systems (such as a chemical system) can be modeled by the addition of terms  $\square_2 \bar{A}_2 \square_3 \bar{A}_3$ ,  $\square_3 \bar{A}_3 \square_1 \bar{A}_1$ , and  $\square_1 \bar{A}_1 \square_2 \bar{A}_2$ , respectively, to Eq. (6).<sup>13</sup> However, the additional terms will not change the conclusions presented here. In fact, purely on the basis of their group structure, it can be shown that whenever a hexagonal array is stable, there is a stable rhombic array close to the same parameters.

The envelope functions given by (5) satisfy (6) with  $A_1 = a_1 = \text{const}$  and  $A_2 = A_3 = a_2 = \text{const}$ , where  $a_1$  and  $a_2$  are solutions of

$$\begin{aligned} \mu a_1 + \alpha a_2^2 - a_1(a_1^2 + 2\rho a_2^2) &= 0, \\ \mu - \gamma \left( \frac{\sqrt{3}}{2} \beta + \frac{\beta^2}{2k_0} \right)^2 + \alpha a_1 - (1 + \rho)a_2^2 - \rho a_1^2 &= 0. \end{aligned} \quad (7)$$

This model based purely on symmetries leads to some surprising predictions that can be tested by experiment. One immediate consequence of the form of the envelope functions (i.e.,  $|A_2| = |A_3| \neq |A_1|$ ) is that the spatial Fourier transform for the rhombic state will contain three pairs of peaks, and that the magnitude of one pair will differ from the other two. This result, which is a consequence of the spatial derivatives, was indeed observed in previous experiments on reaction-diffusion patterns<sup>18</sup> and in numerical simulations of a reaction-diffusion system.<sup>19</sup> [For perturbations of the type (3) it can be shown that  $|A_2| = |A_3| < |A_1|$ . If the hexagonal pattern is stretched along the  $y$  axis, then  $|A_2| = |A_3| > |A_1|$ .]

For given values of  $\rho$ ,  $\alpha$ , and  $\gamma$  there is a finite range of  $\mu$  for which hexagons are stable. The model (6) predicts that for values of  $\mu$  in this stability domain, different rhombic arrays can coexist with hexagons. The characteristic angles of the stable rhombic patterns lie within an interval. Rhombic arrays whose characteristic angle is outside this interval will be unstable and will evolve by spontaneous generation of defects.

The domain of linear stability of the rhombic solution (5) is evaluated by spectral decomposition. The rhombic pattern is perturbed to  $\tilde{A}_1 = a_1 + (u_1 + iv_1)$ ,  $\tilde{A}_2 = [a_2 + (u_2 + iv_2)]e^{i\beta x}$  and  $\tilde{A}_3 = [a_2 + (u_3 + iv_3)]e^{-i\beta x}$ , and the perturbations  $u_n$  (and  $v_n$ ) are expanded as  $u_n = u_n^{(0)} e^{\omega t + i\mathbf{K} \cdot \mathbf{x}}$ . Then (6) reduces to a matrix equation relating  $\omega$  and  $\mathbf{K}$ . The domain of linear stability is the set of

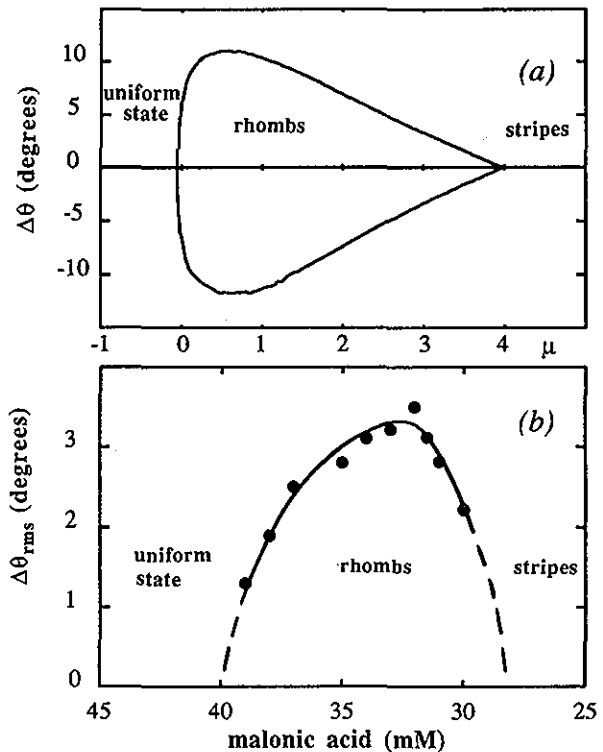


FIG. 2. Predicted and observed bifurcation diagrams. (a) The band of allowed values of  $\Delta\theta$  for linearly stable rhombic arrays as a function of the bifurcation parameter  $\mu$ . The range of  $\Delta\theta$  depends on the values of  $\alpha$ ,  $\rho$ , and  $\gamma$  (here chosen to be 1, 2, and 1, respectively). The bifurcation from the uniform state to rhombic arrays and the bifurcation from rhombic arrays to stripes are both slightly subcritical. (b) The root-mean-square width of the distribution,  $\Delta\theta_{\text{rms}}$ , of angles observed in the reaction-diffusion patterns as a function of the bifurcation parameter, the malonic acid concentration in reservoir B.<sup>9</sup>

parameters  $\mu$  and  $\beta$  for which  $\omega < 0$  for all  $\mathbf{K}$ . The growth rate  $\omega$  has to be calculated numerically (for  $\mathbf{K} = 0$ , it can be done analytically); the results are presented in Fig. 2(a). We have checked that  $\omega$  is negative for 10 values of  $|\mathbf{K}| < 0.25k_0$  and for 20 directions  $\hat{\mathbf{K}}$ .

Close to the middle of the interval in  $\mu$  where the hexagons are stable there is a relatively wide range of angles characterizing linearly stable rhombic arrays. An experimental pattern evolving from a random initial state can locally settle to any one of the states lying within this range. An array of regular hexagons will in general be observed only at the ends of a stability interval where the width of distribution of allowed angles decreases to zero. The width of the distribution will increase toward the center of the stability domain.

### III. EXPERIMENTS

The theoretical predictions are in good accord with experiments that have been conducted on a chlorite-iodide-malonic acid reaction in a thin disk reactor. The reaction occurs in a polyvinyl alcohol gel disk (0.6 mm thick, 25.4 mm diameter), which is sandwiched between two thin membranes (Anopore from Anotec, 0.06 mm thick) that are in contact with continuously refreshed

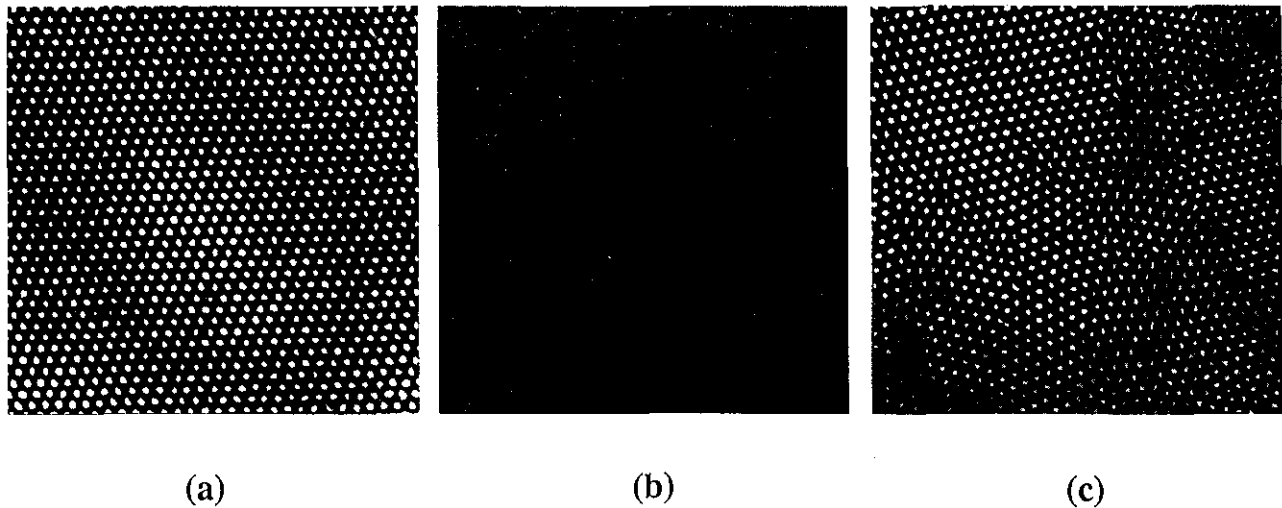


FIG. 3. The evolution of the patterns observed following the removal of a perturbation, which was a perfect rhombic pattern with a characteristic angle of  $50^\circ$ . The imposed pattern was unstable and decayed after the perturbation was removed. The time asymptotic pattern achieved after 20 h has domains with different characteristic angles. The region shown is  $6 \times 6$  mm.<sup>9</sup>

chemical reservoirs.<sup>9</sup> The gel prevents convection but allows for the diffusion of chemicals. The gel also changes the effective diffusion coefficient of iodide by immobilizing the triiodide complex,<sup>20</sup> the latter is dark red and hence serves as a color indicator. The rigid Anopore membrane provides structural support.

A bifurcation from a uniform state to a spatial pattern is observed on decreasing the concentration of one of the feed chemicals (malonic acid). Darker regions in Fig. 1 correspond to regions of high triiodide concentration, the reduced state of the reaction; lighter regions correspond to low triiodide concentration, the oxidized state. After the control parameter value is switched from the spatially uniform regime into a regime where patterns arise, hundreds of target pattern-like light circles appear and grow in a dark background. Within an hour these patterns break up into light stripes and then into a pattern of light dots that evolve more slowly. The distribution of light dots is initially random, but as time evolves the dots organize into many domains of hexagonal and rhombic arrays that are nearly stationary. Boundaries between the domains, visible in Fig. 1(a), move very slowly, typically only a few lattice constants per day.

The robustness of the rhombic patterns was determined in experiments using light as a perturbation (the CIMA reaction is slightly photosensitive). The perturbation was carried out by using a light projector which illuminated the reactor with intense light in a perfect rhombic lattice of dots. The wavelength of the perturbation was carefully chosen to be essentially the same as the intrinsic wavelength determined from spatial Fourier transforms of the unperturbed system. Experiments were conducted with characteristic angles of the rhombic arrays ranging from  $45^\circ$  to  $75^\circ$ . Since the Anopore membrane absorbs all UV light and a large part of the visible light, a long perturbation period (2 to 5 h) was needed. After the perturbation was removed, regular hexagonal patterns were always

found to be stable beyond the bifurcation to patterns. Rhombic patterns with angles within a band near  $60^\circ$  was also stable, but rhombic patterns with angles significantly different from  $60^\circ$  were unstable. Figure 3 shows the evolution of the system following the removal of a perturbation with an unstable rhombic pattern. This supports the prediction of a band of linearly stable rhombic arrays.

Patterns that spontaneously form from the uniform state have multiple domains with different characteristic angles. The root-mean-square width  $\Delta\theta_{\text{rms}}$  of the angular distribution functions, such as those in Fig. 1(c), changes with the bifurcation parameter, as Fig. 2(b) illustrates. This is in good qualitative accord with the theoretical prediction in Fig. 2(a). A quantitative comparison of experiment and theory would require the evaluation of the coefficients in the Landau–Ginzburg equation from the chemical kinetics and diffusion coefficients of the reaction.

#### IV. DISCUSSION

We know of no other laboratory system that has been found to yield rhombic patterns, but the theory is quite general and should apply to other essentially two-dimensional continuum systems.<sup>21</sup> The symmetry assumptions lead to model-independent features that can be checked in experiments, just as we have done with the chlorite–iodide–malonic acid reaction. It will be interesting to see if, nearly a century after Bénard’s discovery of hexagons and Rayleigh’s prediction of convection rolls, another type of periodic pattern is common in these systems. We hope that our work will stimulate a search for rhombic patterns in surface-tension-driven convection, ferrofluids, driven capillary waves, and other systems.

#### ACKNOWLEDGMENTS

We have benefited from discussions with Jacques Boissonade, Pierre Borckmans, Stephen Davis, Patrick De

Kepper, Martin Golubitsky, W. D. McCormick, Ian Melbourne, and Alan Newell. We thank particularly Boris Malomed for helpful discussions. GHG acknowledges partial support from the Energy Laboratory of the University of Houston and from the Office of Naval Research. QO and HLS acknowledge the support of the U.S. Department of Energy Office of Basic Energy Sciences and the Robert A. Welch Foundation.

<sup>1</sup>H. Bénard, *Rev. Gén. Sci. Pures Appl.* **11**, 1261 (1900).

<sup>2</sup>E. L. Koschmieder, *Adv. Chem. Phys.* **26**, 177 (1974).

<sup>3</sup>P. Le Gal, A. Pocheau, and V. Croquette, *Phys. Rev. Lett.* **54**, 2501 (1985).

<sup>4</sup>D. Sornette, *J. Phys. (Paris)* **48**, 151 (1987).

<sup>5</sup>R. E. Rosensweig, *J. Magn. Magn. Mat.* **39**, 127 (1983).

<sup>6</sup>Q. Ouyang and H. L. Swinney, *Nature* **352**, 610 (1991).

<sup>7</sup>Q. Ouyang and H. L. Swinney, *Chaos* **1**, 411 (1991).

<sup>8</sup>In this paper we consider rhombic arrays with characteristic angles near  $60^\circ$ . These patterns are simply referred to as rhombic arrays (following Ref. 19), although a more complete name would be hexagonal arrays deformed along an axis of symmetry.

<sup>9</sup>The concentrations of reservoirs A and B on the opposite sides of the gel were as follows: iodide in both reservoirs, 2.2 mM; sodium sulfate in both reservoirs, 3.0 mM; sulfuric acid in reservoir A (B), 0 (20) mM; chlorite in reservoir A (B), 22 (0) mM; malonic acid in reservoir A (B), 0 (30) mM. In Fig. 1(c) the concentration of malonic acid in reservoir B was 39 mM for the narrow angular distribution, 32 mM for the broad angular distribution. The concentrations are given for the reactant feed stream before any reaction occurs. The reactor was maintained at a temperature of  $5^\circ\text{C}$ .

<sup>10</sup>A. C. Newell, in *Lectures in the Sciences of Complexity*, edited by D. L. Stein (Addison-Wesley, Reading, MA, 1989); A. C. Newell, T. Passot, and J. Lega, *Annu. Rev. Fluid Mech.* **25**, 399 (1993).

<sup>11</sup> $U(x,t)$ , being real, is the sum of the right side and its complex conjugate.

<sup>12</sup>Stretching hexagons along an arbitrary direction leads to a periodic array that can be shown to be stable for small enough deformations. However, symmetry breaking often leads to states that retain most of the original symmetries, and this is perhaps the reason why a rhombic array (which breaks the dihedral symmetry  $D_6$  of the hexagonal array to  $D_2$ ) rather than a general periodic array is seen in experiments. This is the primary motivation for considering only those transformations that stretch the hexagons along an axis of symmetry.

<sup>13</sup>G. H. Gunaratne, *Phys. Rev. Lett.* **71**, 1367 (1993).

<sup>14</sup>E. Buzano and M. Golubitsky, *Philos. Trans. R. Soc. London Ser. A* **308**, 617 (1983).

<sup>15</sup>S. Ciliberto, P. Coulet, J. Lega, E. Pampaloni, and C. Perez-Garcia, *Phys. Rev. Lett.* **65**, 2370 (1990).

<sup>16</sup>For example, see B. A. Malomed, A. A. Nepomnyashchy, and M. I. Tribelskii, *Phys. Rev. A* **42**, 15 (1990).

<sup>17</sup>A. C. Newell and J. A. Whitehead, *J. Fluid. Mech.* **38**, 279 (1969); L. A. Segel, *ibid.* **38**, 203 (1969).

<sup>18</sup>See Fig. 3(c) of Ref. 6 and Fig. 4(c) of Ref. 7. We previously described these patterns as "mixed states." A reexamination of our data reveals that the patterns are rhombs with a characteristic angle  $58^\circ$ .

<sup>19</sup>V. Dufiet and J. Boissonade, *J. Chem. Phys.* **96**, 664 (1992); V. Dufiet and J. Boissonade, *Physica* **188**, 158 (1992).

<sup>20</sup>I. Lengyel, S. Kádár, and I. R. Epstein, *Phys. Rev. Lett.* **69**, 2729 (1992).

<sup>21</sup>The patterns in our system with crossed gradients in a direction normal to the gel disk are essentially two dimensional since the thickness of the pattern is less than or comparable to a wavelength. See Q. Ouyang, Z. Noszticzius, and H. L. Swinney, *J. Phys. Chem.* **96**, 6773 (1992).